Available online at www.sciencedirect.com
ScienceDirect
Surface & Coatings Technology 202 (2008) 2008–2014
SURFACE & COATINGS TECHNOLOGY
www.elsevier.com/locate/surfcoat

The effects of niobium and nickel on the corrosion resistance of the zinc phosphate layers

E.P. Banczek [a,*], P.R.P. Rodrigues [b], I. Costa [a]

[a] *Instituto de Pesquisas Energéticas e Nucleares, IPEN/CNEN-SP, Centro de Ciência e Tecnologia de Materiais, São Paulo, Brazil*
[b] *Universidade Estadual do Centro-Oeste, Departamento de Química/Unicentro-Guarapuava, Brazil*

Received 21 February 2007; accepted in revised form 23 August 2007
Available online 30 August 2007

Abstract

In this investigation the viability of nickel substitution by niobium in zinc phosphate (PZn) baths has been studied. Samples of carbon steel (SAE 1010) were phosphated in two baths, one containing nickel (PZn+Ni) and the other with niobium substituting nickel (PZn+Nb). Potentiodynamic polarization curves (anodic and cathodic, separately) and electrochemical impedance spectroscopy (EIS) were used to evaluate the corrosion resistance of the phosphated carbon steels in a 0.5 mol L^{-1} NaCl electrolyte. The phosphate layers obtained were analysed by X-ray diffraction and it was found that they are composed of $Zn_3(PO_4)_2.4H_2O$ (hopeite) and $Zn_2Fe(PO_4)_2.4H_2O$ (phosphophylite). Surface observation by scanning electron microscopy (SEM) showed that the PZn+Ni layer is deposited as needle-like crystals, whereas the PZn+Nb layer shows a granular morphology. The electrochemical results showed that the PZn+Nb coating was more effective in the corrosion protection of the carbon steel substrate than the PZn+Ni layer. The results also suggested that nickel can be replaced by niobium in zinc phosphate baths with advantageous corrosion properties of the layer formed.

Keywords: Phosphating; Zinc phosphate; Niobium; Nickel; Corrosion; Carbon steel

1. Introduction

Phosphating is one of the most used surface treatments for metallic surfaces [1–10]. It is known as a conversion coating that leads to the formation of insoluble phosphate salts, mainly zinc phosphate [11,12] and is employed in many industries either for corrosion protection, surface preparation for painting, or for decoration [11,12] in a variety of metallic materials. This type of coating can be applied on steels [1–5,7], galvanized steel [4,10,13], iron [6], magnesium [8,14,15], aluminium [9,16] and zinc [17].

There are many types of phosphating baths such as, zinc based [1,17–20], manganese based [4,21–23], tricationic [24], organic phosphate [6,25,26] or even a combination of them. The type of coating used depends on the phosphated material application.

Studies on the phosphating reactions resulted in decreased temperature of the phosphating bath and also in the time of immersion time. This was possible due to variations in the electrical current and phosphating bath composition with the addition of some components to accelerate the phosphating process and also obtaining phosphate layer with better properties [11].

As mentioned above, the electrical current was among the phosphating accelerator agent investigated [2,5,7,17,18] but also the chemical compounds were used. The chemical compounds that act as accelerators might be oxidant compounds or salts of metals nobler than the metal to be phosphated. The use of chemical additives as phosphating accelerator has the advantage of being less costly in comparison to modifications in the current density.

The accelerators act as: (i) depolarizers of the surface reactions, mainly those of high electronic density (microcathodes), and (ii) oxidant of the metal cations on the microanodes leading to the precipitation of insoluble phosphate salts [11].

Various types of chemical accelerators for phosphating can be used such as sodium nitrite [1,7,14,27–29], nitrates [3,7,8,14,15,27,28,30,31] and chlorates [30,32]. Besides the chemical accelerator other additives are used to afford other

* Corresponding author. Avenida Prof. Lineu Prestes, 2242, CEP 05508-900, São Paulo, SP, Brazil. Tel.: +55 11 3816 9356; fax: +55 11 3816 9370.
E-mail address: ebanczek@ipen.br (E.P. Banczek).

0257-8972/$ - see front matter © 2007 Elsevier B.V. All rights reserved.
doi:10.1016/j.surfcoat.2007.08.039

specific properties. Various additives are used such as calcium ions [7,32–35], manganese ions [19,21,23,30,35–37], tartaric acid [8,15], fluoride ions [8,14–16,27,29], nickel ions [1,16,19,28,30,32,38], copper ions [39] molybdenum ions [15,37] and, more recently, niobium [39].

The present work aims to evaluate the viability of nickel substitution by niobium in zinc phosphate baths, as an environmental friendly alternative to the commercial phosphating processes usually adopted.

2. Experimental

2.1. Sample preparation

The material used as substrate was a carbon steel (SAE 1010) (composition in Table 1) from which samples with 10 × 15 × 2 mm were cut and then phosphated.

The samples surfaces for phosphating were prepared by SiC grinding with SiC emery paper in the sequence #220, #320, #400 and #600, respectively. After grinding, the samples were degreased in a commercial alkaline solution for 5 min at (70 ± 5) °C and then, rinsed. Subsequently, the samples were immersed in an alkaline solution titanated with a commercial compound, that is, a titanium phosphate salt in the concentration of 3 g/L (pH = 7.5–9.0), for 90 s at (25 ± 2) °C for surface activation. Next, the samples were immersed in the phosphating bath either with nickel (PZn + Ni) or niobium (PZn + Nb), for 5 and 3 min respectively, at (25 ± 2) °C, and then dried and weighed, obtaining m_1. The determination of the deposited phosphate layer weight was carried out by solubilization of the phosphate layer in a 0.5 g/L chromium trioxide for 15 min at (75 ± 5) °C, followed by weighing, obtaining m_2. The phosphate layer weight ($m_{phosphate}$) was estimated by Eq. (1):

$$m_{phosphate} = \frac{m_1 - m_2}{A} \quad (1)$$

where m_1 is the phosphated steel weight, m_2 is the steel weight after phosphate layer solubilization, and A is the surface area exposed to the phosphating bath.

Concentrated solutions for phosphating, either with Ni (PZn + Ni) or with Nb (PZn + Nb) addition, were prepared and their main composition is shown in Table 2. A niobium compound was prepared by alkaline fusion of 1 g of Nb_2O_5 and 5 g KOH, as described in [40]. Nb was added to one of the concentrated phosphate solutions shown in Table 2 by addition of 0.5 g of the alkaline fusion compound obtained. The Zn, Ni and Nb content in the concentrated solutions was determined by Induced Coupled Plasma Optical Emission Spectroscopy (ICP OES). From the concentrated solutions, the phosphating baths were prepared by dilution and addition of sodium hydroxide (NaOH 50%). The phosphating baths were titrated of the diluted phosphating bath with NaOH 0.1 mol L^{-1}. The total and free acidity values were 28 and 1.6 points, respectively.

Sodium nitrite ($NaNO_2$) was used as an accelerator in the phosphating bath at concentrations of 0.5 g/L, for the PZn + Ni bath, and 2 g/L for the PZn + Nb one.

All the solutions were prepared with analytical grade chemical compounds and deionized water.

Table 1
Chemical composition of carbon steel (SAE 1010) used as substrate for phosphating

Element	Composition (wt.%)
C	0.118
Si	0.023
Mn	0.310
P	0.020
S	0.016
Cr	0.024
Ni	0.028
Mo	0.002

Table 2
Chemical composition of concentrated phosphate bath

Component (g/L)	PZn + Ni	PZn + Nb
H_3PO_4	521.4	521.4
HNO_3	363.3	363.3
Zn	185.8	168.9
Ni	4.24	–
Nb	–	0.136
H_2O_2	0.032	0.032
H_2O(mL)	434.4	440.7

2.2. Characterization of the phosphate layers

The morphology of the phosphate layers obtained was evaluated by Scanning Electron Microscopy (SEM) using a Philips XL30 microscope and their thickness was determined by thickness measurements at 10 areas of 3 different samples.

The phases in the phosphate layer were investigated by X-ray diffraction analysis (XDR) with a diffractometer Rigaku DEMAX 2000 using radiation of CuKα (1.5418 Å).

The coating roughness was determined according to JIS 2001 standard using a roughness meter Mitutoyo Surftest J-301 series at 10 areas of 3 different samples.

The electrochemical behaviour of the phosphated samples was evaluated by potentiodynamic polarization (anodic and cathodic) measurements and electrochemical impedance spectroscopy (EIS), using a frequency response analyser (Gamry model EIS 300) coupled to a potenciostat PCI4/300. Working electrodes with an area of 1.5 cm^2 were used in the electrochemical tests. A platinum wire and a silver/silver chloride electrode were used as counter and reference electrodes, respectively. A sodium chloride solution (0.5 mol L^{-1} NaCl; pH = 6.0) was used for electrochemical characterization of the phosphate layer. The electrolyte was quiescent, naturally aerated and at (20 ± 2) °C.

Potentiodynamic polarization tests were carried out from the corrosion potential E_{corr} up to an overpotential of ±400 mV, using a scanning rate of 1 mVs^{-1}.

The EIS measurements were potentiostatically performed at E_{corr}, with a perturbation amplitude of ± 10 mV in the frequency

range from 100 kHz to 10 mHz, using an acquisition rate of 10 points per decade.

3. Results and discussion

3.1. Phosphate layer weight

The average weight of the phosphate layers obtained at various times of immersion in the two phosphating baths time are shown in Fig. 1.

The average weight of the coating obtained in the PZn+Nb bath is higher and time for stabilization is lower than that in the PZn+Ni one. This could be explained by the higher concentration of accelerating agent ($NaNO_2$) in the Nb containing bath in comparison to that without this additive. The immersion times for phosphate deposition in PZn+Ni and PZn+Nb baths were 5 and 3 min, respectively. These immersion periods are necessary for weight stabilization, as it can be observed in Fig. 1.

3.2. Characterization of phases in the phosphate layer

The phases in the phosphate layers obtained in the types of baths used were analysed by X-ray diffraction analysis and the results are shown in Fig. 2. The phases present in the phosphate layers were mainly $Zn_3(PO_4)_2{\cdot}4H_2O$ (hopeite) and $Zn_2Fe(PO_4)_2{\cdot}4H_2O$ (phosphophylite).

According to literature [11,41] phosphating of metallic substrates occurs through the following reactions:

$$Me_{(s)} + 2H^+ \rightarrow Me^{2+} + H_{2(g)} \quad (1)$$

$$3Zn^{2+} + 2H_2PO_4^- + 4H_2O \rightarrow Zn_3(PO_4)_2.4H_2O + 4H^+ \quad (2)$$

$$Fe^{2+} + 2Zn^{2+} + 2H_2PO_4^- + 4H_2O \rightarrow Zn_2Fe(PO_4)_2.4H_2O + 4H^+ \quad (3)$$

The first reaction corresponds to the metal attack by the acid phosphating solution and the two following reactions lead to phosphate crystals formation and deposition on the metallic surface.

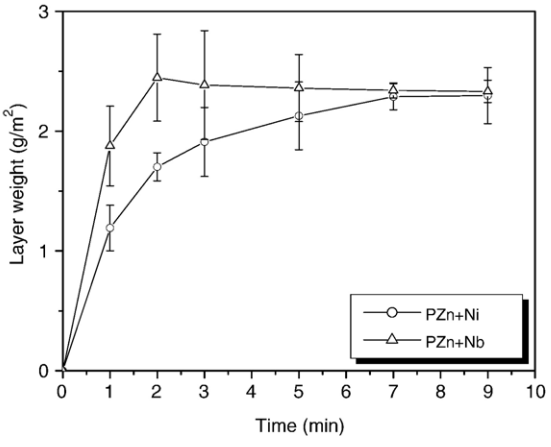

Fig. 1. Average weight of phosphate layer obtained at various time of immersion in the two phosphating baths.

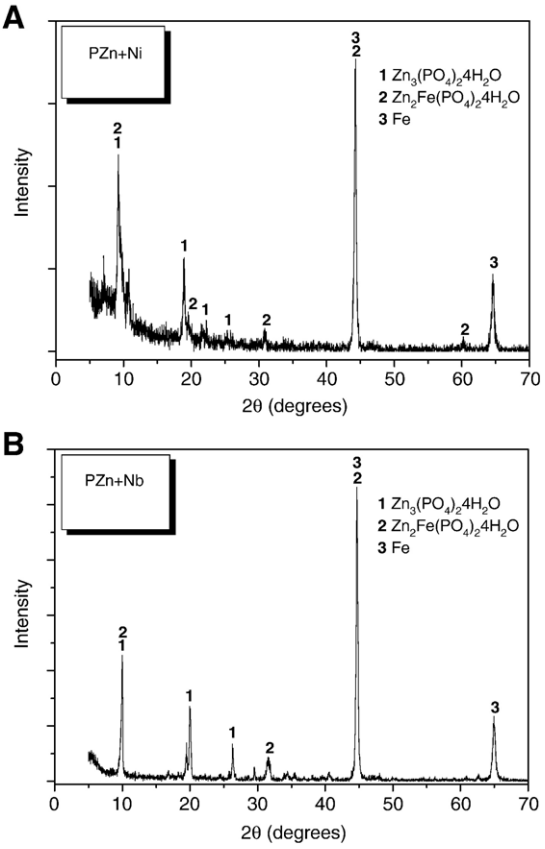

Fig. 2. X-ray diffractogram of the surface layer after immersion in (A) PZn+Ni and (B) PZn+Nb baths.

3.3. Morphology characterization of the phosphate layers

The phosphate layers morphology was evaluated by scanning electron microscopy (SEM) and the micrographs obtained are shown in Fig. 3. The phosphate layer obtained in the PZn+Ni bath (Fig. 3 (B)), shows needle-like crystals, whereas that obtained in the PZn+Nb bath shows granular morphology, that promote a better surface coverage. This suggests that the layer obtained in the PZn+Nb bath, leads to better corrosion resistance than that in the PZn+Ni one.

3.4. The effect of Nb addition

The $NaNO_2$ concentration usually adopted for activation in phosphating baths is 0.5 g/L [1,8,38,39]. Phosphating in the PZn+Nb bath with 0.5 g/L $NaNO_2$ however, led to phosphate deposition on only few areas of the metallic substrate, as Fig. 4 shows. The micrograph of Fig. 4 clearly shows that most of the carbon steel substrate immersed in the Nb containing phosphating bath was uncovered. It is likely that the substitution of Ni by Nb promotes the metallic surface passivation hindering the phosphate layer deposition.

To evaluate the effect of Nb on the surface passivation, a carbon steel sample was phosphated in baths without either, nickel and niobium, and the results are shown in Fig. 5.

A comparison of the carbon steel surfaces immersed in phosphating baths of similar composition, either with or without

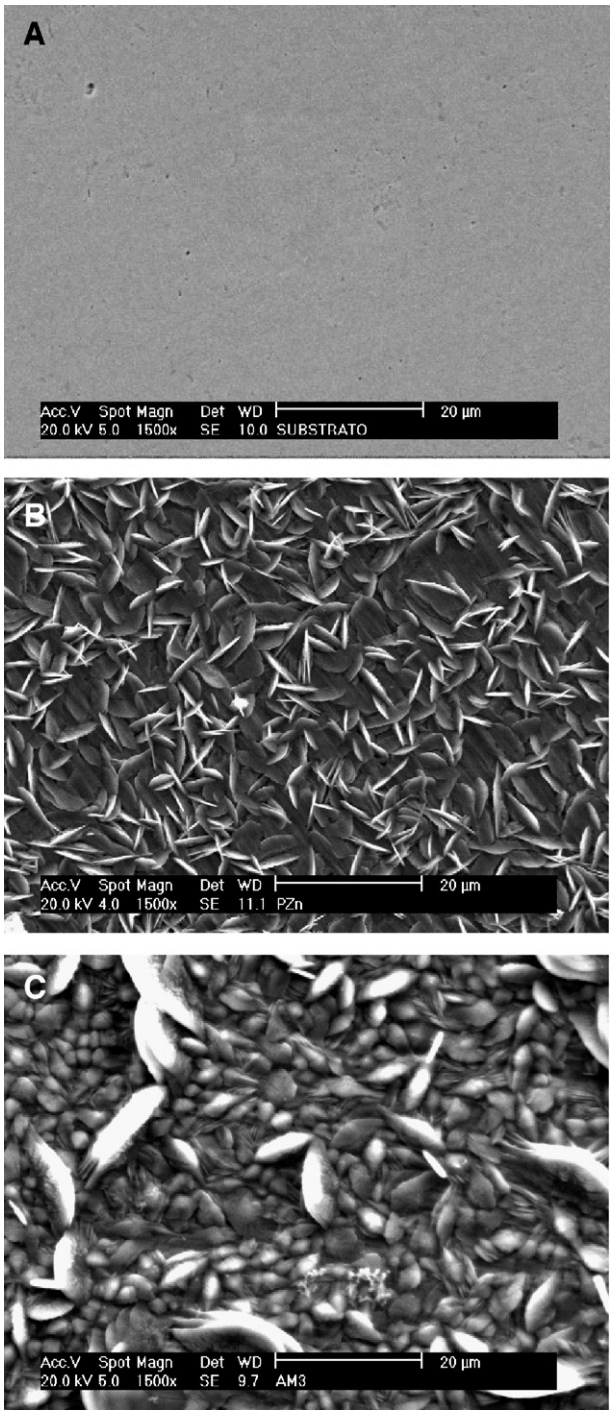

Fig. 3. Micrographs of the carbon steel (SAE 1010) surface prior to (A) and after phosphating in (B) PZn+Ni bath ($NaNO_2$=0.5 g/L;T=25 °C, t=5 min), and (C) PZn+Nb, ($NaNO_2$=2 g/L, T=25 °C, t=3 min).

Nb, Figs. 4 and 5, respectively, shows that in the solution without Nb, the carbon steel surface was phosphate coated and this suggests that Nb hinders the phosphating process.

The time of immersion and the $NaNO_2$ concentration were varied to evaluate their effect on phosphating and the results are shown in Fig. 6.

The immersion time in the phosphating bath had no significant effect on the surface coverage (Figs. 4 and 6 (A)).

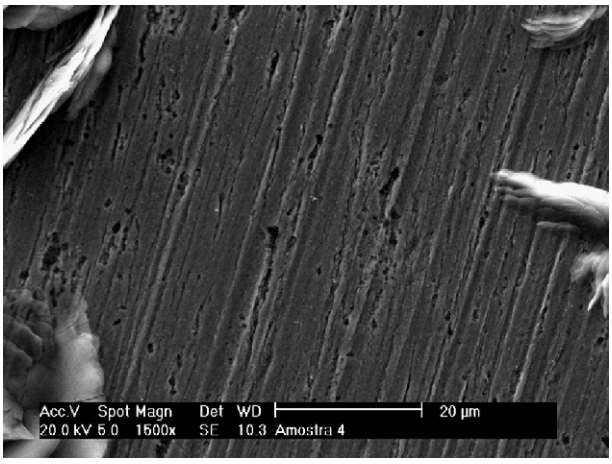

Fig. 4. Micrograph of carbon steel (SAE 1010) after phosphating in the PZn+Nb solution ([$NaNO_2$]=0.5 g/L, T=25 °C, t=5 min).

On the other hand, the $NaNO_2$ concentration had a clear influence on phosphating and consequently on surface coverage (Fig. 6 (B)). The surface coverage increased with $NaNO_2$ concentration, and it was completely covered when the $NaNO_2$ concentration was 2 g/L, as Fig. 6 (C) shows.

Although high $NaNO_2$ concentrations (2 g/L) in phosphating baths can generate higher amounts of rejects, the literature [14,27] reports on phosphate layers obtained in solutions with 3 g/L of $NaNO_2$ concentration.

3.5. Phosphate layer thickness evaluation

The phosphate layer thickness was evaluated by means of SEM on the cross section areas of phosphated steel which are shown in Fig. 7. It is clearly seen that the phosphate layer obtained in the PZn+Nb bath is thicker than that in the PZn+Ni one.

The mean thickness values for both phosphate layers, PZn+Ni and PZn+Nb, were (23.4±1.89) µm and (28.5±3.78) µm, respectively, suggesting that the last layer could provide better corrosion resistance to carbon steel substrate.

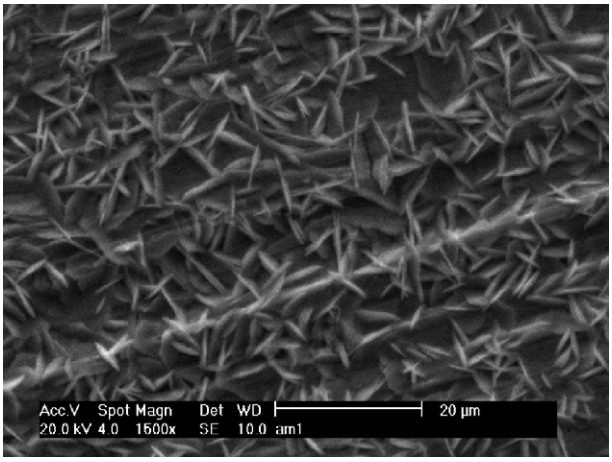

Fig. 5. Micrograph of the carbon steel (SAE 1010) after being phosphating in a bath without Ni or Nb ([$NaNO_2$]=0.5 g/L, T=25 °C, t=5 min).

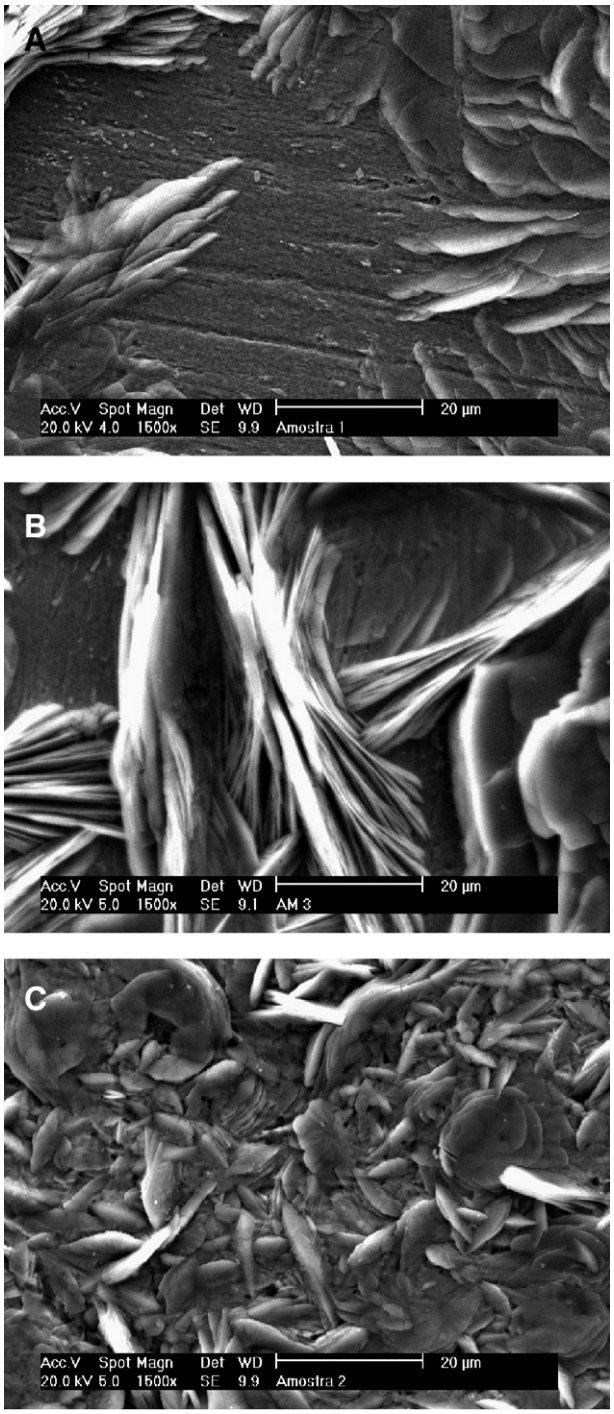

Fig. 6. SEM micrographs of carbon steel (SAE 1010) surface phosphated in:(A) PZn+Nb ([$NaNO_2$]=0.5 g/L, T=25 °C, t=10 min; (B) PZn+Nb, ([$NaNO_2$]= 1 g/L, T=25 °C, t=5 min; and (C) PZn+Nb, ([$NaNO_2$]=2 g/L, T=25 °C, t=5 min).

3.6. Surface roughness evaluation

The surface roughness of the phosphate layers is a very important parameter of the surface as it affects paint adhesion. Paint adhesion is favored in rougher surfaces as it helps paint anchorage.

The results showed that the phosphate layer obtained in PZn+Nb solution presents higher roughness (0.371±0.078) µm than that in PZn+Ni (0.251±0.048) µm one. A possible reason for this result is the higher number of crystals deposited on the steel surface immersed in the Nb containing solution. A comparison of the micrographs shown in Fig. 3 (B) and (C), supports this hypothesis. Better adhesion between the phosphate layer and organic coatings would be therefore expected for the samples phosphated in the PZn+Nb solution.

3.7. Electrochemical characterization

The anodic polarization curves corresponding to bare and phosphated carbon steel samples are shown in Fig. 8.

A typical passive behavior is found for the phosphated samples at low overpotentials. A large current density increase is however seen at potentials around −450 mV and −350 mV for the samples phosphated in PZn+Ni and PZn+Nb, respectively. These results indicate a slight better resistance of the layer obtained in the PZn+Nb bath compared to the PZn+Ni. The reasons for this behavior could be related to the higher thickness and coverage of the first layer. Consequently, these better phosphate layer properties lead to better corrosion resistance of the phosphated steel.

Cathodic polarization curves were also obtained in NaCl 0.5 mol L^{-1} solution and these are shown in Fig. 9.

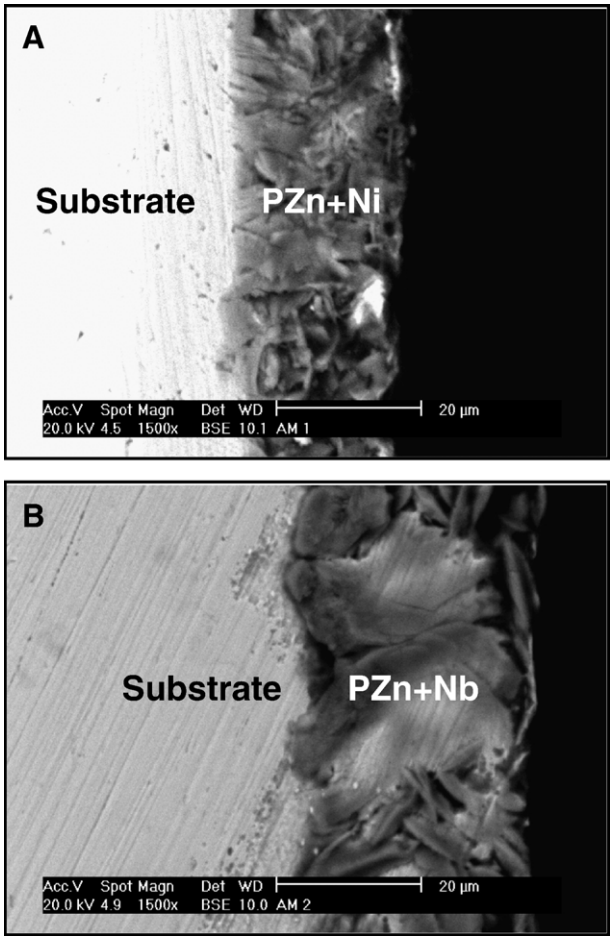

Fig. 7. Cross section of the phosphated carbon steel (SAE 1010) showing the thickness of the layers obtained in: (A) PZn+Ni and (B) PZn+Nb baths.

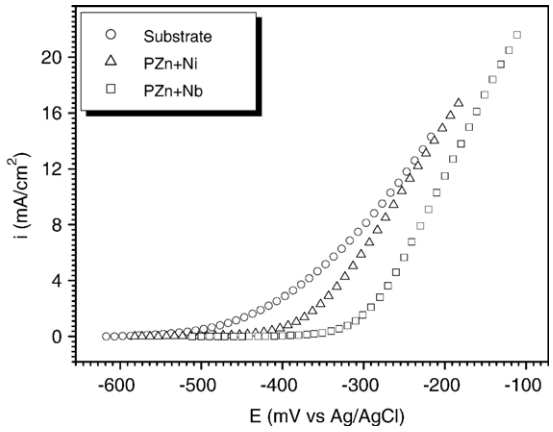

Fig. 8. Anodic polarization curves of bare and phosphated carbon steel (SAE 1010), obtained in NaCl 0.5 mol L^{-1} solution.

For all cathodic polarization curves a limit current density (i_L) was found showing that the cathodic reaction is diffusion controlled. The i_L values decreased for the phosphated steels as compared to the bare steel, and the lowest i_L value was associated to the PZn+Nb phosphated steel showing that the phosphate layer obtained in the Nb contain bath polarized the cathodic reaction.

The corrosion current density values (i_{corr}) were estimated from extrapolation of the linear region of the cathodic curve to the corrosion potential (E_{corr}). The mean i_{corr} and E_{corr} values were estimated from four polarization curves and the results are presented in Table 3. The corrosion inhibiting efficiency (θ) was estimated by Eq. (2):

$$\theta = \frac{i^o_{corr} - i_{corr}}{i^o_{corr}} \times 100 \quad (2)$$

where:

$i_{corr}{}^o$ corrosion rates of substrate
i_{corr} corrosion rates of coated substrate

The results demonstrate that the phosphate layers lead to corrosion potential increase to nobler values, suggesting that

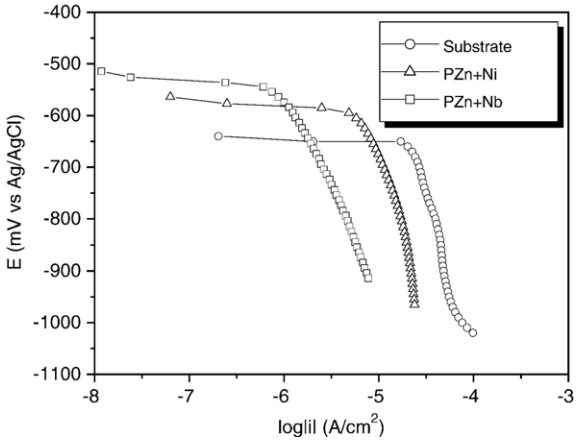

Fig. 9. Cathodic polarization curves of bare and phosphated carbon steel (SAE 1010), obtained in NaCl 0.5 mol L^{-1} solution.

Table 3
Mean values of i_{corr}, E_{corr} and corrosion inhibiting efficiency (θ) obtained from the cathodic polarization curves

Sample	i_{corr} (μA/cm²)	E_{corr} (V)	θ (%)
Substrate	28.3±3.25	−0.597±0.02	–
PZn+Ni	5.33±1.32	−0.555±0.09	81±2.2
PZn+Nb	1.69±0.53	−0.527±0.12	95±1.9

besides affecting the cathodic reaction, this layer also has a significant influence on the anodic reaction, as it was indicated in Fig. 8. A higher efficiency was associated to the phosphate layer obtained in the PZn+Nb bath, as the previous results had indicated.

The electrochemical impedance spectroscopy (EIS) results obtained in NaCl 0.5 mol L^{-1} solution are shown in Fig. 10 as Nyquist (A) and Bode phase angle (B) diagrams. For the carbon steel only a time constant is indicated. A phase angle peak is seen on the Bode diagram at approximately 1 Hz, whose time constant must be associated to charge transfer reactions. The Nyquist diagrams of the phosphated steels show two capacitive arcs suggesting two time constants, whereas the Bode diagrams show a large peak from the high frequencies to approximately 10 Hz, indicating the interaction

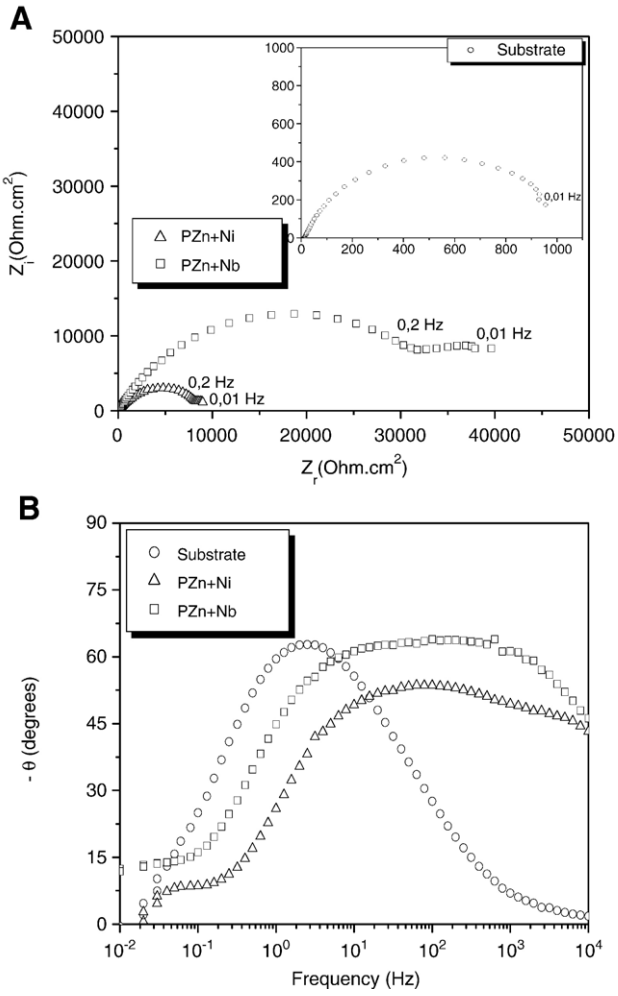

Fig. 10. (A) Nyquist and (B) Bode phase angle diagrams obtained in NaCl 0.5 mol L^{-1} solution for bare and phosphated carbon steel (SAE 1010).

of the time constants. At lower frequencies another phase angle peak is seen.

The large peak at higher frequencies (1000 Hz) for the phosphated samples is associated to the pores resistance to electrolyte penetration. Phase angles at the high frequencies are higher for the layer obtained in PZn+Nb comparatively to than obtained in PZn+Ni, supporting the previous results that indicate better corrosion protection properties associated to the first type of layer. The higher impedance values associated to this layer also supports this indication.

The phase angle peak at 0.1 Hz for the phosphated samples is attributed to the substrate–electrolyte interface interaction underneath the phosphate layer [1]. The interaction of this low frequency time constant with the higher frequency one is indicated on the diagrams.

The EIS results supported the polarization measurements and indicated that the layer obtained in the Nb containing bath was more effective against corrosion than in the PZn+Ni one.

4. Conclusions

The gravimetric analysis showed increased mass deposition associated to the phosphate layer obtained in PZn+Nb than in the PZn+Ni. Also, the time for weight stabilization and consequently complete formation of phosphate layer was lower for the PZn+Nb solution than for the PZn+Ni one. This result indicates faster, higher and consequently more economical phosphating process associated to the first type of phosphate layer.

The X-ray diffraction analysis showed that the main phases found in the phosphate layers obtained in the two types of phosphating baths used were $Zn_3(PO_4)_2.4H_2O$ (hopeite) and $Zn_2Fe(PO_4)_2.4H_2O$ (phosphophylite).

The SEM micrographs showed that the layer formed in PZn+Ni bath consists of needle-like crystals, whereas the morphology of the layer formed in the PZn+Nb solution is composed of grain-like crystals that result in enhanced surface coverage than the needle-like type. Improved surface coverage must lead to better corrosion resistance. The results also showed that the phosphate layer obtained in the PZn+Nb bath is thicker and rougher than that in the PZn+Ni one.

The electrochemical characterization of the phosphate layers obtained showed better corrosion resistance and, consequently, higher efficiency associated to the phosphate layer deposited in the PZn+Nb comparatively to that in the PZn+Ni one. From the results of the present study it can be concluded that Nb can substitute Ni in phosphating baths with economical advantages.

Acknowledgements

The authors are grateful to FAPESP and CNPq for the financial support provided to this research and also to CBMM for the Nb_2O_5 used in this study.

References

[1] E.P. Banczek, P.R.P. Rodrigues, I. Costa, Surf. Coat. Technol. 201 (2006) 3701.
[2] S. Jegannathan, T.S.N. Sankara Narayanan, K. Ravichandran, S. Rajeswari, Surf. Coat. Technol. 200 (2006) 6014.
[3] Chao-Min Wang, Han-Chih Liau, Wen-Ta Tsai, Surf. Coat. Technol. 201 (2006) 2994.
[4] T. K Rout, H.K. Pradhan, T. Venugopalan, Surf. Coat. Technol. 201 (2006) 3496.
[5] S. Jegannathan, T.S.N. Sankara Narayanan, K. Ravichandran, S. Rajeswari, Surf. Coat. Technol. 200 (2006) 4117.
[6] S. Rebeyrat, J.L. Grosseau-Poussard, J.F. Silvain, B. Panicaud, J.F. Dinhut, Appl. Surf. Sci. 199 (2002) 11.
[7] P.T. Olesen, T. Steenberg, E. Christensen, N.J. Bjerrum, J. Mater. Sci. 33 (1998) 3059.
[8] L.Y. Niu, Z.H. Jiang, G.Y. Li, C.D. Gu, J.S. Lian, Surf. Coat. Technol. 200 (2006) 3021.
[9] M.C. Whitten, C-Tsu Lin, Prog. Org. Coat. 38 (2000) 151.
[10] G. Bustamante, F.J. Fabri-Miranda, I.C.P. Margarit, O.R. Mattos, Prog. Org. Coat. 46 (2003) 84.
[11] V. Gentil, Corrosion, LTC3th edition, 1987, p. 319, (In Portuguese).
[12] G. Lorin, Phosphating of Metals, Finishing Publications, Ltd., Middlesex1974, p. 4.
[13] H.A. Ponte, A.M. Maul, E.A. Alvarenga, Mater. Res. 4 (2002) 439.
[14] L. Kouisni, M. Azzi, M. Zertoubi, F. Dalard, S. Maximovitch, Surf. Coat. Technol. 185 (2004) 58.
[15] J.S. Lian, G.Y. Li, L.Y. Niu, C.D. Gu, Z.H. Jiang, Q. Jiang, Surf. Coat. Technol. 200 (2006) 5956.
[16] A.S. Akhtar, D. Susac, P. Glaze, K.C. Wong, K.A.R. Mitchell, Surf. Coat. Technol. 187 (2004) 208.
[17] S. Jegannathan, T.S.N. Sankara Narayanan, K. Ravichandran, S. Rajeswari, Electrochem. Acta 51 (2005) 247.
[18] T.S.N.S. Narayanan, S. Jegannathan, K. Ravichandran, Prog. Org. Coat. 55 (2006) 355.
[19] M. Shoeib, M. Farouk, F. Hanna, Met. Finish. (Sept. 1997) 62.
[20] M. Wolpers, J. Angeli, Appl. Surf. Sci. 179 (2001) 281.
[21] D. Weng, P. Jokiel, A. Uebleis, H. Boehni, Surf. Coat. Technol. 88 (1996) 147.
[22] Y. Totik, Surf. Coat. Technol. 200 (2004) 2711.
[23] J. Flis, J. Mankowski, T. Zakroczymski, T. Bell, Corros. Sci. 43 (2001) 1711.
[24] E.P. Banczek, M.F. Oliveira, M.T. Cunha, P.R.P. Rodrigues, Port. Electrochim. Acta 23 (2005) 379.
[25] B. Ptacek, F. Dalard, J.J. Rameau, Surf. Coat. Technol. 82 (1996) 277.
[26] L. Gang, S. Wangen, C. Yanrong, Z. Shili, Met. Finish. (Sept. 1997) 54.
[27] L. Kouisni, M. Azzi, F. Dalard, S. Maximovitch, Surf. Coat. Technol. 192 (2005) 239.
[28] D. Zimmermann, A.G. Munoz, J.W. Schultze, Electrochem. Acta 48 (2003) 3267.
[29] D. He, F. Chen, A. Zhou, L. Nie, S. Yao, Thin Solid Films 382 (2001) 263.
[30] G.Y. Li, J.S. Lian, L.Y. Niu, Z.H. Jiang, Q. Jiang, Surf. Coat. Technol. 201 (2006) 1814.
[31] L.C. Deepa, S. Sathiyanarayanan, C. Marikkannu, D. Mukherjee, Anti-Corros. Methods Mater. 4 (2003) 286.
[32] G. Górecki, Met. Finish. (March 1995) 36.
[33] P.K. Sinha, R. Feser, Surf. Coat. Technol. 161 (2002) 158.
[34] G. Bikulcius, V. Burokas, A. Martusiene, E. Matulionis, Surf. Coat. Technol. 172 (2003) 139.
[35] S. Palraj, M. Selvaraj, P. Jayakrishnan, Prog. Org. Coat. 54 (2005) 5.
[36] P. Hivart, B. Hauw, J.P. Bricout, J. Oudin, Tribol. Int. 8 (1997) 561.
[37] G. Li, L. Niu, J. Lian, Z. Jiang, Surf. Coat. Technol. 176 (2004) 215.
[38] D. Zimmermann, A.G. Munoz, J.W. Schultze, Surf. Coat. Technol. 197 (2005) 260.
[39] E.P. Banczek, P.R.P. Rodrigues, I. Costa, Proceedings of 29th Annual Congress of the Brazilian Chemical Society, Águas de Lindóia, São Paulo, Brazil2006, p. 107, (In Portuguese).
[40] BR n. PI 0602009-7, 18 Jul. 2006, Manufacture of niobium soluble compounds for metallic surface treatments, Universidade Estadual do Centro-Oeste. (In Portuguese).
[41] E. Tegehall, Colloids Surf. Coat. 49 (1990) 373.